

Nuclear Force from Lattice QCD

N. Ishii^{1,2}, S. Aoki^{3,4} and T. Hatsuda²

¹ Center for Computational Sciences, University of Tsukuba, Tsukuba 305-8577, Ibaraki, JAPAN,

² Department of Physics, University of Tokyo, Tokyo 113-0033, JAPAN,

³ Graduate School of Pure and Applied Sciences,

University of Tsukuba, Tsukuba 305-8571, Ibaraki, JAPAN and

⁴ RIKEN BNL Research Center, Brookhaven National Laboratory, Upton, New York 11973, USA

Nucleon-nucleon (NN) potential is studied by lattice QCD simulations in the quenched approximation, using the plaquette gauge action and the Wilson quark action on a 32^4 ($\simeq (4.4 \text{ fm})^4$) lattice. A NN potential $V_{\text{NN}}(r)$ is defined from the equal-time Bethe-Salpeter amplitude with a local interpolating operator for the nucleon. By studying the NN interaction in the $^1\text{S}_0$ and $^3\text{S}_1$ channels, we show that the central part of $V_{\text{NN}}(r)$ has a strong repulsive core of a few hundred MeV at short distances ($r \lesssim 0.5 \text{ fm}$) surrounded by an attractive well at medium and long distances. These features are consistent with the known phenomenological features of the nuclear force.

PACS numbers: 12.38.Gc, 13.75.Cs, 21.30.Cb

More than 70 years ago, Yukawa introduced the pion to account for the strong interaction between the nucleons (the nuclear force) [1]. Since then, enormous efforts have been devoted to understand the nucleon-nucleon (NN) interaction at low energies both from theoretical and experimental points of view. As shown in Fig.1, phenomenological NN potentials are thought to be characterized by three distinct regions [2, 3]: The long range part ($r \gtrsim 2 \text{ fm}$) is well understood and is dominated by the one pion exchange. The medium range part ($1 \text{ fm} \lesssim r \lesssim 2 \text{ fm}$) receives significant contributions from the exchange of multi-pions and heavy mesons (ρ , ω , and σ). The short range part ($r \lesssim 1 \text{ fm}$) is empirically known to have strong repulsive core [7], which is essential not only for describing the NN scattering data, but also for the stability and saturation of atomic nuclei, for determining the maximum mass of neutron stars, and for

igniting the Type II supernova explosions [8]. Although the origin of the repulsive core must be closely related to the quark-gluon structure of the nucleon, it has been a long-standing open questions in QCD [9].

In this Letter, we report our first serious attempt to attack the problem of nuclear force from lattice QCD simulations [10]. The essential idea is to define a NN potential from the equal-time Bethe-Salpeter (BS) amplitude of the two local interpolating operators separated by distance r [11]. This type of BS amplitude has been employed by CP-PACS collaboration to study the $\pi\pi$ scattering on the lattice [12]. As we shall see below, our NN potential shows a strong repulsive core of about a few hundred MeV at short distances surrounded by an attraction at medium and long distances in the s-wave channel.

Let us start with an effective Schrödinger equation obtained from the BS amplitude for two nucleons at low energies [12, 13]:

$$-\frac{1}{2\mu}\nabla^2\phi(\vec{r}) + \int d^3r' U(\vec{r}, \vec{r}')\phi(\vec{r}') = E\phi(\vec{r}), \quad (1)$$

where $\mu \equiv m_N/2$ and E is the reduced mass of the nucleon and the non-relativistic energy, respectively. For the NN scattering at low energies, the non-local potential U is represented as $U(\vec{r}, \vec{r}') = V_{\text{NN}}(\vec{r}, \nabla)\delta(\vec{r}-\vec{r}')$ with the derivative expansion [2]: $V_{\text{NN}} = V_{\text{C}}(r) + V_{\text{T}}(r)S_{12} + V_{\text{LS}}(r)\vec{L} \cdot \vec{S} + O(\nabla^2)$. Here $S_{12} = 3(\vec{\sigma}_1 \cdot \hat{r})(\vec{\sigma}_2 \cdot \hat{r}) - \vec{\sigma}_1 \cdot \vec{\sigma}_2$ is the tensor operator with $\hat{r} \equiv |\vec{r}|/r$, \vec{S} the total spin operator, and $\vec{L} \equiv -i\vec{r} \times \vec{\nabla}$ the relative angular momentum operator. The central NN potential $V_{\text{C}}(r)$, the tensor potential $V_{\text{T}}(r)$ and the spin-orbit potential $V_{\text{LS}}(r)$ can be further decomposed into various spin-isospin channels, e.g. $V_{\text{C}}(r) = V_{\text{C}}^1(r) + V_{\text{C}}^\sigma(r)\vec{\sigma}_1 \cdot \vec{\sigma}_2 + V_{\text{C}}^\tau(r)\vec{\tau}_1 \cdot \vec{\tau}_2 + V_{\text{C}}^{\sigma\tau}(r)(\vec{\sigma}_1 \cdot \vec{\sigma}_2)(\vec{\tau}_1 \cdot \vec{\tau}_2)$. In the phenomenological analysis of the NN scattering phase shift [3], the Schrödinger equation with a certain parametrization of V_{NN} is solved and compared with the data. On the other hand, if we

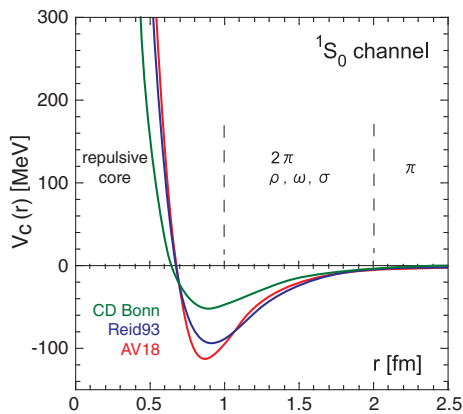


FIG. 1: Three examples of the modern NN potential in the $^1\text{S}_0$ (spin singlet and s-wave) channel: CD-Bonn [4], Reid93 [5] and AV18 [6] from the top at $r = 0.8 \text{ fm}$.

can calculate $\phi(\vec{r})$ directly from lattice simulations for various E , Eq.(1) can be used to define the non-local potential $U(\vec{r}, \vec{r}')$ directly without recourse to the experimental inputs except for quark masses and the QCD scale parameter. In this Letter, instead of finding U by varying E , we take only the leading term in the derivative expansion at low energies and extract the central potential $V_C(r)$ at fixed E through

$$V_C(r) = E + \frac{1}{2\mu} \frac{\vec{\nabla}^2 \phi(r)}{\phi(r)}. \quad (2)$$

On the lattice, $\phi(\vec{r})$ with zero angular momentum ($\ell = 0$) is defined from the equal-time BS amplitude as

$$\begin{aligned} \phi(\vec{r}) \equiv & \frac{1}{24} \sum_{\mathcal{R} \in O} \frac{1}{L^3} \sum_{\vec{x}} \\ & \times P_{ij}^\tau P_{\alpha\beta}^\sigma \left\langle 0 \left| N_\alpha^i(\mathcal{R}[\vec{r}] + \vec{x}) N_\beta^j(\vec{x}) \right| \text{NN} \right\rangle, \end{aligned} \quad (3)$$

where we choose the local interpolating operator for the nucleon: $N_\alpha^i = \epsilon_{abc} ({}^t q^a C \gamma_5 \tau_2 q^b) q_\alpha^{i,c}$ with a, b and c the color indices, α and β the Dirac indices, i and j the isospin indices, and $C \equiv \gamma_4 \gamma_2$ the charge conjugation. \vec{r} describes the spatial separation between the nucleons. Since we consider the NN scattering at low energies, we take only the upper components of N_α^i . The summation over the vector \vec{x} projects out the state with zero total-momentum. The summation over discrete rotation \mathcal{R} of the cubic group O projects out the A_1^+ representation which contains $\ell = 0$ state and $\ell \geq 4$ states. The former can be singled out by selecting the lowest energy state with the procedure given in Eq.(4). The spin (isospin) projection is carried out by the operator P^σ (P^τ); for example, $P_{\alpha\beta}^\sigma = (\sigma_2)_{\alpha\beta} (= \delta_{\alpha\beta})$ in the spin-singlet (spin-triplet) channel. The renormalization factor Z , which relates the BS amplitude on the lattice and that in the continuum, cancels out in $V_C(r)$.

The $\phi(\vec{r} = \vec{y} - \vec{x})$ in Eq.(3) is nothing but the probability amplitude to find ‘‘nucleonlike’’ three quarks located at point \vec{x} and another ‘‘nucleonlike’’ three quarks located at point \vec{y} . In terms of the physical states, $\phi(\vec{r})$ contains not only the elastic amplitude $\text{NN} \rightarrow \text{NN}$ but also the inelastic amplitudes such as $\text{NN} \rightarrow \pi \text{NN}$. However, at low energies below threshold, the inelastic part is spatially localized and does not affect the asymptotic form of $\phi(\vec{r})$. Note also that a different choice of the nucleon interpolating operator modifies the relative weight of the elastic and inelastic amplitudes and thus leads to a different NN potential. Nevertheless, they give the same scattering phase shift since the asymptotic form of $\phi(\vec{r})$ is independent of the interpolating operators. It is an open question at the moment how the short distant structure of V_{NN} to be shown below is affected by the change of the interpolating operator. For more details on these points, see [13].

In the actual simulations, Eq. (3) is obtained through the four point nucleon correlator,

$$\begin{aligned} F_{\text{NN}}(\vec{x}, \vec{y}, t; t_0) \equiv & \left\langle 0 \left| N_\alpha^i(\vec{x}, t) N_\beta^j(\vec{y}, t) \overline{\mathcal{J}}_{\text{NN}}(t_0) \right| 0 \right\rangle \\ = & \sum_n A_n \left\langle 0 \left| N_\alpha^i(\vec{x}) N_\beta^j(\vec{y}) \right| n \right\rangle e^{-E_n(t-t_0)}. \end{aligned} \quad (4)$$

Here $\overline{\mathcal{J}}_{\text{NN}}(t_0)$ is a source term located at $t = t_0$, which produces the nucleons with zero total momentum. To enhance the ground state contribution of the NN system, we adopt the wall source, $\mathcal{J}_{\text{NN}}(t_0) = P_{ij}^\tau P_{\alpha\beta}^\sigma \mathcal{N}_\alpha^i(t_0) \mathcal{N}_\beta^j(t_0)$, where \mathcal{N} is obtained from N by replacing q by $Q(t_0) = \sum_{\vec{x}} q(\vec{x}, t_0)$. E_n is the energy of the two-nucleon state $|n\rangle$ and $A_n(t_0) \equiv \langle n | \overline{\mathcal{J}}_{\text{NN}}(t_0) | 0 \rangle$. Because of the finite lattice volume L^3 , the energy E takes discrete value and has a finite shift from the non-interacting case $\Delta E = O(1/L^3)$ to be determined from the simulations [14].

In this Letter, we focus on the spin-singlet and spin-triplet channels with zero orbital angular momentum. In the standard notation, the former (latter) corresponds to the ${}^{2s+1}\ell_J = {}^1S_0$ ($= {}^3S_1$) channel, where s, ℓ and J denote the total spin, orbital angular momentum, and the total angular momentum of the two nucleons. The 1S_0 is the simplest channel where only the central potential $V_C(r)$ contributes. On the other hand, there arises a mixing between the 3S_1 and 3D_1 channels because of the tensor force $V_T(r)$. In this case, one may define an effective central potential $V_C^{\text{eff}}(r)$ which consists of the bare central potential and the induced central potential by the 3D_1 admixture [2]. The definition in Eq.(2) with $\phi(\vec{r})$ being projected onto 1S_0 (3S_1) corresponds to the central potential (the effective central potential).

To calculate $\phi(\vec{r})$, we have carried out simulations on a 32^4 lattice in the quenched approximation. We employ the plaquette gauge action with the gauge coupling $\beta = 5.7$ and the Wilson quark action. The lattice spacing

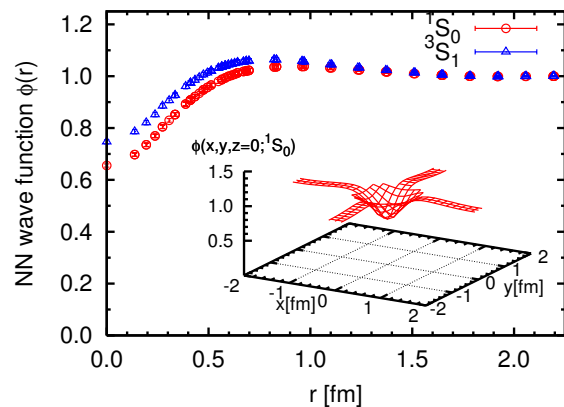


FIG. 2: The lattice QCD result of the radial dependence of the NN wave function at $t-t_0 = 6$ in the 1S_0 and 3S_1 channels. Inset shows the two-dimensional view in the $x-y$ plane.

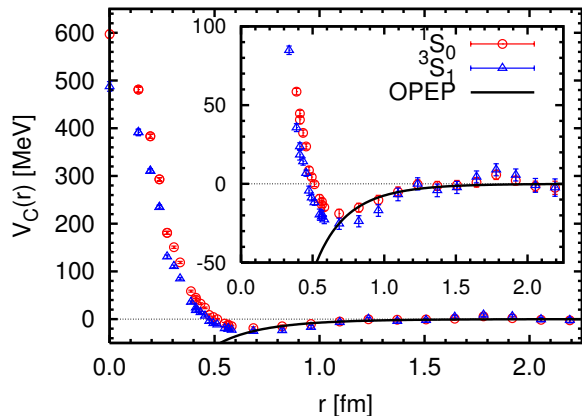


FIG. 3: The lattice QCD result of the central (effective central) part of the NN potential $V_C(r)$ ($V_C^{\text{eff}}(r)$) in the 1S_0 (3S_1) channel for $m_\pi/m_\rho = 0.595$. The inset shows its enlargement. The solid lines correspond to the one-pion exchange potential (OPEP) given in Eq.(5).

determined from the ρ meson mass in the chiral limit is $a^{-1} = 1.44(2)$ GeV ($a \simeq 0.137$ fm) [15], which leads to the lattice size $(4.4 \text{ fm})^4$. The hopping parameter is chosen to be $\kappa = 0.1665$, which corresponds to $m_\pi \simeq 0.53$ GeV, $m_\rho \simeq 0.89$ GeV and $m_N \simeq 1.34$ GeV. We use the global heat-bath algorithm with overrelaxations to generate the gauge configurations. After skipping 3000 sweeps for thermalization, 500 gauge configurations are collected with the interval of 200 sweeps. Results for lighter and heavier quark masses with higher statistics will be reported in [13]. The Dirichlet (periodic) boundary condition for quarks is imposed in the temporal (spatial) direction. To avoid the boundary effect, the wall source is placed at $t = t_0 = 5$ at which the Coulomb gauge fixing is made. The ground state saturation for $t - t_0 \geq 6$ is checked by the effective mass of the two-nucleon system.

Fig. 2 shows the lattice QCD result of the wave function at the time-slice $t - t_0 = 6$. They are normalized at the spatial boundary $\vec{r} = (32/2 = 16, 0, 0)$. All the data including the off-axis ones are plotted for $r \lesssim 0.7$ fm, beyond which we plot only the data locating on the coordinate axes and their nearest neighbors. As is clear from Fig. 2, the wave function is suppressed at short distance and have a slight enhancement at medium distance, which suggests that the NN system has a repulsion (attraction) at short (medium) distance.

Fig. 3 shows the central (effective central) NN potential in the 1S_0 (3S_1) channel at $t - t_0 = 6$. As for ∇^2 in Eq. (2), we take the discrete form of the Laplacian with the nearest-neighbor points. E is obtained from the Green's function $G(\vec{r}; E)$ which is a solution of the Helmholtz equation on the lattice [12]. By fitting the wave function $\phi(\vec{r})$ at the points $\vec{r} = (10 - 16, 0, 0)$ and $(10 - 16, 1, 0)$ by $G(\vec{r}; E)$, we obtain $E(^1S_0) = -0.49(15)$

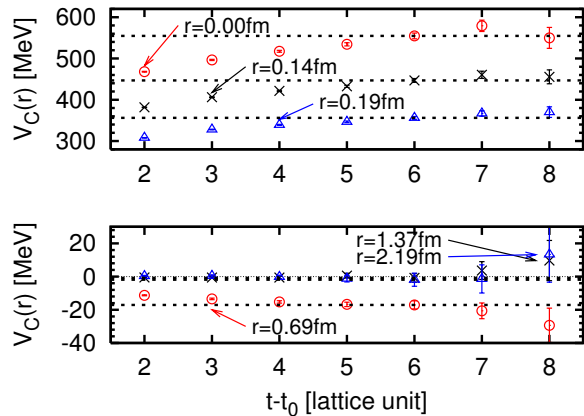


FIG. 4: $t - t_0$ dependence of $V_C(r)$ in the 1S_0 channel for several different values of the distance r .

MeV and $E(^3S_1) = -0.67(18)$ MeV. Namely, there is a slight attraction between the two nucleons in a finite box. To make an independent check of the ground state saturation, we plot the t dependence of $V_C(r)$ in the 1S_0 channel at several distances $r = 0, 0.14, 0.19, 0.69, 1.37$ and 2.19 fm in Fig. 4. The saturation indeed holds for $t - t_0 \geq 6$ within errors.

As anticipated from Fig. 2, $V_C(r)$ and $V_C^{\text{eff}}(r)$ have repulsive core at $r \lesssim 0.5$ fm with the height of about a few hundred MeV. Also, they have an attraction of about $-(20-30)$ MeV at the distance $0.5 \lesssim r \lesssim 1.0$ fm. The solid lines in Fig. 3 show the one pion exchange contribution to the central potential calculated from

$$V_C^\pi(r) = \frac{g_{\pi N}^2}{4\pi} \frac{(\vec{\tau}_1 \cdot \vec{\tau}_2)(\vec{\sigma}_1 \cdot \vec{\sigma}_2)}{3} \left(\frac{m_\pi}{2m_N} \right)^2 \frac{e^{-m_\pi r}}{r}, \quad (5)$$

where we have used $m_\pi \simeq 0.53$ GeV and $m_N \simeq 1.34$ GeV to be consistent with our data, while the physical value of the πN coupling constant is used, $g_{\pi N}^2/(4\pi) \simeq 14.0$. Even in the quenched approximation, the one pion exchange is possible as the connected quark exchange between the two nucleons. In addition, there is in principle a quenched artifact to the NN potential from the flavor-singlet hairpin diagram (the ghost exchange) between the nucleons [16]. Its contribution to the central potential reads [18]: $V_C^\eta(r) = \frac{g_{\eta N}^2}{4\pi} \frac{\vec{\sigma}_1 \cdot \vec{\sigma}_2}{3} \left(\frac{m_\pi}{2m_N} \right)^2 \left(\frac{1}{r} - \frac{m_0^2}{2m_\pi} \right) e^{-m_\pi r}$. Here $g_{\eta N}$ and m_0 are the ηN coupling constant and a mass parameter of the ghost, respectively. The ghost potential has an exponential tail which dominates over the Yukawa potential at large distances. Its significance can be estimated by comparing the sign and the magnitude of $e^{m_\pi r} V_C(r)$ and $e^{m_\pi r} V_C^{\text{eff}}(r)$ at large distances, because $V_C^\eta(r)$ has an opposite sign between 1S_0 and 3S_1 . Our present data shows no evidence of the ghost at large distances within errors, which may indicate $g_{\eta N} \ll g_{\pi N}$.

Several comments are in order here:

1. The asymptotic wave function at low energy ($E \rightarrow 0$) is approximated as $\phi_{\text{asy}}(r) = \frac{\sin(kr + \delta_0(k))}{kr} \rightarrow \frac{r + a_0}{r}$, where $\delta_0(k)$ (a_0) is the s-wave scattering phase shift (scattering length). From the zero of $r\phi_{\text{asy}}(r)$, we find $a_0(^1S_0) = 0.066(22)$ fm and $a_0(^3S_1) = 0.089(27)$ fm under the assumption that $E \sim -0.5$ MeV is small enough [19]. The reason of having such a small a_0 is easily understood from the well-known formula in the Born approximation: $a_0 \simeq -m_N \int_0^\infty V_C(r)r^2 dr$, where (i) the volume factor $r^2 dr$ hides the repulsive core at short distances, and (ii) a_0 is a subtle quantity which suffers from a large cancellation between repulsion and attraction.
2. The above points (i) and (ii) also provide a reason why it is dangerous at the moment to compare a_0 obtained in unphysical quark masses with a_0 in experiments [17]. A slight change of the depth and height of the potential by the change of the quark mass may affect the scattering length substantially.
3. If the attraction becomes large enough at small m_π , the system may have a bound state and a_0 changes sign from positive to negative. In the real world, this happens in 3S_1 (the deuteron channel). Indeed, the inset of Fig. 3 shows that 3S_1 has stronger attraction than 1S_0 . Note that this difference cannot be attributed to the ghost contribution, because it is repulsive (attractive) in 3S_1 (1S_0).
4. Our preliminary result with the lighter quark mass at $\kappa = 0.1678$ ($m_\pi \simeq 0.36$ GeV, $m_\rho \simeq 0.84$ GeV and $m_N \simeq 1.2$ GeV) [13] shows that the height of the repulsive core increases by 40 % at the origin, while the minimum of the potential is shifted to $r \sim 0.8$ fm with approximately the same depth.

In summary, we have studied the NN interaction using the lattice QCD simulations in the quenched approximation on a $(4.4 \text{ fm})^4$ lattice with the quark mass corresponding to $m_\pi/m_\rho = 0.595$. We define a NN potential with the use of the equal-time Bethe-Salpeter amplitude for two local interpolating operators of the nucleon. The central (effective central) part of the potential in the 1S_0 (3S_1) channel at low energies turns out to have a repulsive core at short distances surrounded by attractive well at medium and long distances. These properties are known to be the important features of the phenomenological NN potential. The long range tails of $V_C(r)$ in both channels are consistent with the one-pion exchange within statistical errors. We did not find numerical evidence of the ghost exchange (quenched artifact) for $m_\pi/m_\rho = 0.595$. Preliminary calculation with the lighter quark mass ($m_\pi/m_\rho = 0.433$) shows that the short range repulsion becomes stronger and the range of the potential becomes wider.

It would be quite interesting to derive the tensor and spin-orbit forces by making appropriate projections of the wave function. Studies of the hyperon-nucleon and hyperon-hyperon potentials, whose experimental information is currently very limited, are now under investi-

gation: They are particularly important for the physics of hyper nuclei and neutron star core. To unravel the physical origin of the repulsive core, we need further studies on its quark mass dependence, channel dependence and interpolating-operator dependence. Also, the full QCD simulations at the physical quark mass are necessary to be done in the future.

The authors thank N. Ishizuka, H. Nemura, D. Kaplan, U. van Kolck, R. Machleidt, S. Sasaki, M. Savage, and M. Hjorth-Jensen for useful comments. N.I. thanks N. Shimizu for useful information and discussions. This research was supported in part by the Grant-in-Aid of MEXT (Nos. 13135204, 15540251, 15540254, 18540253). Our simulations have been performed with IBM Blue Gene/L at KEK under a support of its Large Scale Simulation Program, No.18 and No.06-21 (FY2006).

-
- [1] H. Yukawa, Proc. Math. Phys. Soc. Japan, **17**, 48 (1935).
 - [2] M. Taketani et al., Prog. Theor. Phys. Suppl. **39**, 1 (1967); **42**, 1 (1968).
 - [3] R. Machleidt and I. Slaus, *J. Phys.* **G27**, R69 (2001).
 - [4] R. Machleidt, Phys. Rev. C **63**, 024001 (2001).
 - [5] V. G. J. Stoks, R. A. M. Klomp, C. P. F. Terheggen and J. J. de Swart, Phys. Rev. C **49**, 2950 (1994).
 - [6] R. B. Wiringa, V. G. J. Stoks and R. Schiavilla, Phys. Rev. C **51**, 38 (1995).
 - [7] R. Jastrow, Phys. Rev. **81**, 165 (1951).
 - [8] H. Heiselberg and V. Pandharipande, Ann. Rev. Nucl. Part. Sci. **50**, 481 (2000);
 - [9] M. Oka, K. Shimizu and K. Yazaki, Prog. Theor. Phys. Suppl. **137**, 1 (2000).
 - [10] For preliminary data on a $(2.2 \text{ fm})^3 \times (3.3 \text{ fm})$ lattice, see N. Ishii, S. Aoki and T. Hatsuda, hep-lat/0610002 [*Proceedings of Science LAT2006*, 109 (2006)]
 - [11] For a different method introducing heavy quark(s) to define the distance r , see, D. Arndt, S. R. Beane and M. J. Savage, Nucl. Phys. A **726** (2003) 339; T.T. Takahashi, T. Doi and H. Suganuma, hep-lat/0601006 [*AIP Conf. Proc.* **842**, 249 (2006)]
 - [12] S. Aoki et al. (CP-PACS Coll.), Phys. Rev. **D71** (2005) 094504.
 - [13] The derivation of the effective Schrödinger equation and its relation to half off-shell T-matrix as well as high statistics lattice QCD simulations with lighter quark mass will be reported elsewhere: N. Ishii, S. Aoki and T. Hatsuda, paper in preparation.
 - [14] M. Lüscher, Nucl. Phys. B **354**, 531 (1991).
 - [15] M. Fukugita, Y. Kuramashi, M. Okawa, H. Mino, A. Ukawa, Phys. Rev. **D52**, 3003 (1995).
 - [16] S.R. Beane, M.J. Savage, Phys. Lett. **B535**, 177 (2002).
 - [17] S.R. Beane, P.F. Bedaque, K. Orginos and M.J. Savage, Phys. Rev. Lett. **97**, 012001 (2006).
 - [18] With another ghost parameter α_Φ , the formula is modified as $1/r \rightarrow (1 - \alpha_\Phi)/r$ and $m_0^2 \rightarrow m_0^2 - \alpha_\Phi m_\pi^2$.
 - [19] The Lüscher's finite volume formula [14] together with E obtained in the text lead to $a_0(^1S_0) = 0.123(39)$ fm and $a_0(^3S_1) = 0.17(5)$ fm, which are consistent with those obtained from the wave function.